Simulation and Experiments of an *S*-Band 20-kW Power-Adjustable Phase-Locked Magnetron

Heping Huang, Yu Wei, Xiaojie Chen, Kama Huang, *Senior Member, IEEE*, and Changjun Liu, *Senior Member, IEEE*

***Abstract*— A 3-D particle-in-cell simulation model of a commercial industrial heating magnetron is developed as a guide for improving a fixed-output-power magnetron. After this improvement, the magnetron is transformed into a 20-kW power-adjustable phase-locked magnetron, which can then be injection-locked with tunable power output. For the first-time ever, the output power of the injection-locked magnetron is continuously tuned from 2 to 19 kW. This large-power magnetron is both phase and amplitude controlled, and is useful for the coherent power combining of multiple magnetrons. The magnetron frequency pushing effect, which affects the injection-locked frequency range of the phase-locked magnetron, is observed in both simulations and measurements. In the injection-locking experiments, the locking bandwidth varies from 11.7 to 2.4 MHz when the output power is tuned from 5 to 19.1 kW and the injection power is kept at 120 W. Moreover, the center frequency of the phase-locked magnetron increases with increasing output power.**

***Index Terms*— Continuous-wave (CW) magnetron, particle-in-cell (PIC) simulation, phase-locking bandwidth, power adjustable.**

I. Introduction

MAGNETRONS are classical electric-magnetic crossed-field nonlinear oscillator devices [1], [2], which have been extensively used in industrial applications (including microwave drying and microwave heating [2]), owing to their high efficiency, low cost, and environmental friendliness. Large-power continuous-wave (CW) industrial magnetrons have been applied in a few new areas (for example, the microwave plasma chemical vapor deposition method) [3]. In large-scale industrial applications, magnetron microwave sources yield significant reduction in system costs, such as in Space Solar Power Satellite (SSPS) [4], [5], and high-power magnetron transmitters [6]. The power capacity of a single magnetron is typically inadequate for large-power industrial applications. A large-power microwave source can be obtained by combining the power of multiple magnetrons. However, a normal CW magnetron is characterized by a complex frequency and hence, obtaining a high efficiency is difficult when the power of various magnetrons is combined [7]. This drawback may be overcome by using injection-locking technology, which stabilizes the amplitude of, and renders tunable, the output signal from the magnetron.

Injection-locked magnetrons have been studied for many years, and successfully applied to the locking of relativistic magnetrons [8]–[10]. The injection-locking of CW magnetrons has attracted increasing attention, owing to the recent development of important applications including microwave power transmission, SSPS, and high-power magnetron transmitters [11]–[13]. In general, investigations of injection-locked magnetrons have focused mainly on phase control (rather than on power adjustment). In 2004, Shinohara and Matsumoto [5], [14] successfully developed a 300 to 500 W phase and amplitude controlled magnetron for microwave power transmission. This represented the first-ever application where the phase and amplitude of an injection-locked magnetron were simultaneously tuned. Moreover, Tahir *et al.* [15] used a 1.2-kW oven magnetron as a current-controlled oscillator. In our previous work, we realized coherent power combining, which phase tuning, of two 15-kW fixed-output-power injection-locked magnetrons [16]. The applications and academic work of magnetron operation have been done for many years [2]. However, experimental phenomena associated with magnetron operations remain unclear. With the development of simulation technology, some of these phenomena may be understood by comparing experimental and simulation results [17].

In industrial applications, power-adjustable microwave sources are essential for avoiding microwave heating disasters (for example, thermal runaway) and improving the heating efficiency. In this paper, we improved the direct current (dc) power supply of a magnetron, using the simulation results of a computer simulation technology (CST) 3-D particle-in-cell (PIC) model as a guide for the improvements. These improvements transform a fixed-output-power magnetron into a 20-kW power-adjustable magnetron system, which is a large-power, phase and amplitude controlled system. The scheme of the experiment system reform consists mainly of rebuilding the switched-mode customized power supply of the magnetron. The magnetron power-adjustable simulation and experiments are presented in Section II. Frequency pushing will influence the injection-locked frequency range of the phase-locked magnetron, and therefore, the frequency pushing effect and the phenomena occurring in the magnetron during the simulation are considered in Section III. Moreover, the injection-locked

Manuscript received December 31, 2016; revised March 14, 2017; accepted March 21, 2017. Date of publication April 14, 2017; date of current version May 8, 2017. This work was supported in part by the China 973 program under Grant 2013CB328902 and in part by the National Natural Science Foundation of China under Grant 61271074. *(Corresponding Author: Changjun Liu.)*

The authors are with the School of Electronics and Information Engineering, Sichuan University, Chengdu 610064, China (e-mail: cjliu@ieee.org).

Color versions of one or more of the figures in this paper are available online at http://ieeexplore.ieee.org.

Digital Object Identifier 10.1109/TPS.2017.2689502

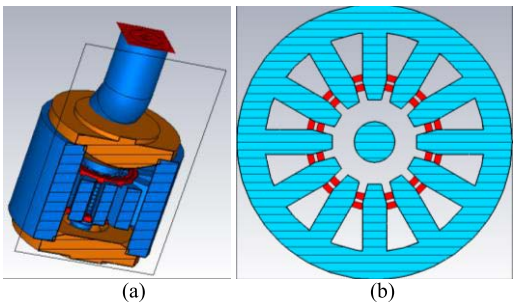

Fig. 1. Simulation model. (a) 3-D model of the magnetron. (b) 12 sector-and-slot side resonator.

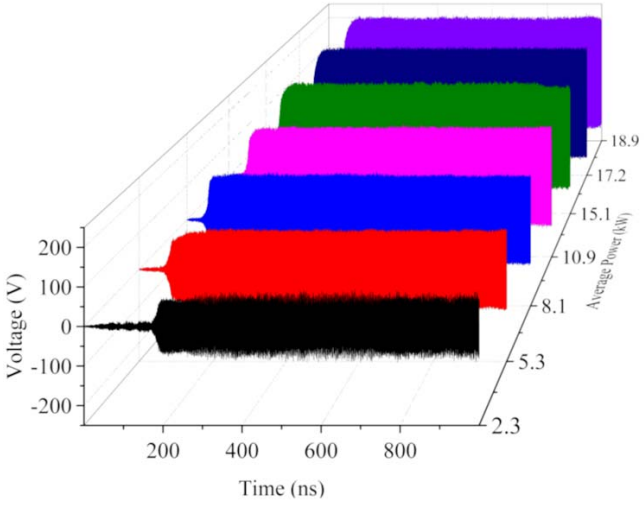

Fig. 2. Magnetron simulation output at various values of the output power.

magnetron simulation and experimental measurement data are presented in Section IV. The conclusion is given in Section V.

II. Simulations and Experiments on Free-Running Power-Adjustable Magnetron

A. Simulation of the Magnetron in Free-Running Mode

A CST 3-D PIC model, as shown in Fig. 1(a), is set up using the actual magnetron cavity dimensions. The magnetron consists of 12 sector-and-slot side resonators. Four straps are applied to both sides of the anode vanes, as shown in Fig. 1(b). The output antenna is also included in the model. Fixed simulation dc high voltage and magnetic field intensity of 11.4 kV and 1550 Gs, respectively, are considered, whereas the operating current is adjustable. We obtain a pi-mode oscillation in the resonator at this operating point. A simulation is performed at each value of the operating current and results, including the time-domain output, spectrum, particle numbers, and spoke figures, are obtained. The average power and anode current are calculated from the particle collision data.

The output signal and free-running spectra obtained at various anode currents are shown in Figs. 2 and 3, respectively. Each curve is associated with an overall simulation time of 1000 ns, and the magnetron is started up at the beginning. When the oscillation mode is stable, the simulation of the magnetron is also stable.

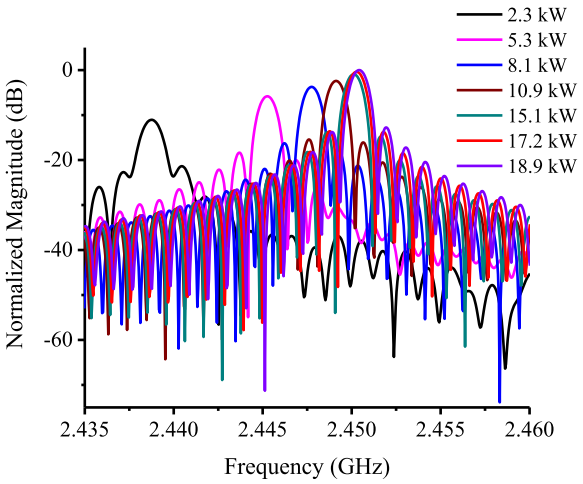

Fig. 3. Magnetron oscillating spectrum at various values of the output power.

Fig. 4. Water-cooled CW 20-kW magnetron.

TABLE I
Free-Oscillation Experiment Measurement Results

Anode Current (A)	Frequency (GHz)	Filament Current (A)	Output Power (kW)
0.40	2.434	42.1	2.30
0.70	2.442	41.4	5.27
1.00	2.447	37.8	8.12
1.44	2.449	33.8	11.2
1.88	2.450	29.5	15.2
2.14	2.450	26.9	17.4
2.30	2.450	25.1	18.9

When the operating dc high voltage and the magnetic field intensity are almost constant, the anode current gives rise to frequency pushing, as shown in Fig. 3. The frequency increases from 2.438 to 2.502 GHz with increasing anode current.

B. Experimental Results

An *S*-band water-cooled CW magnetron (Nanjing Sanle Microwave Technology Development Co., Ltd; see Fig. 4) is used in the experiments, and the switched-mode power supply of this industrial heating magnetron is rebuilt. In the experiments, the operating cathode voltage of the magnetron and the electromagnetic current are fixed at approximately −11.4 kV and 3.2 A, respectively, and the magnetic field intensity is 1550 Gs. The almost constant dc high voltage of the magnetron is generated by the switched-mode power supply, which provides an adjustable anode current supply and filament current supply.

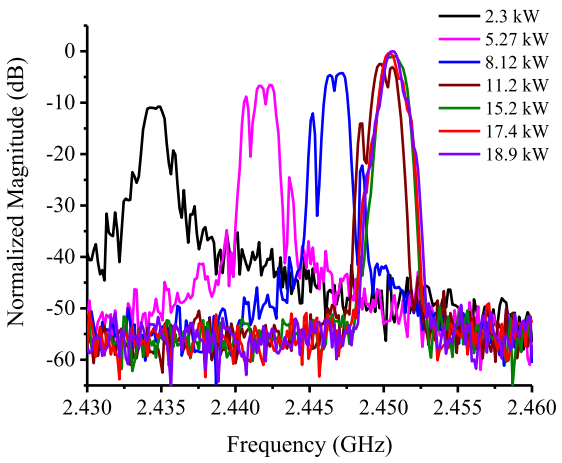

Fig. 5. Experimental measurement results of the spectrum at various output power.

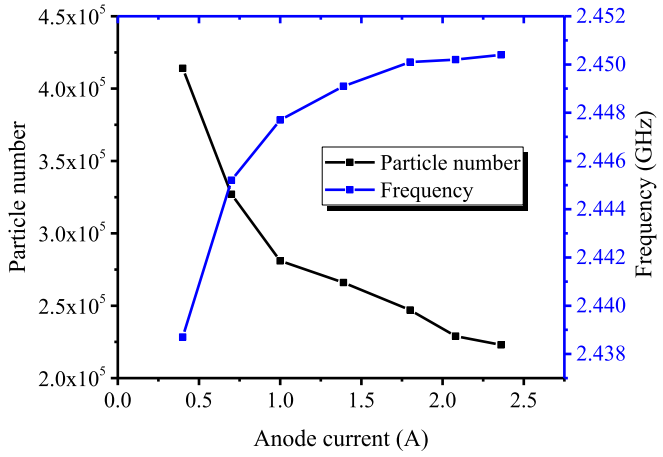

Fig. 6. Dependence of the oscillating frequency and the number of particles on the anode current.

Fig. 5 shows the spectra obtained at various values of the output power. The data obtained from the free-oscillation measurements are shown in Table I. During the experiment, we adjust the anode current such that various values of the output power (which is continuously tuned from 2 to 19 kW)are realized. At high output power, the filament current must be reduced for continued proper functioning of the magnetron. A frequency shift occurs in all experiments, but the frequency (of the magnetron) becomes increasingly stable when the output power reaches ~70% of the switching power supply.

III. Frequency Pushing Effects

Frequency pushing means that the frequency increases with increasing anode current of the magnetron [1]. For constant operating dc high voltage and magnetic field intensity during the simulation, we investigate magnetron pushing and the formation of an electron bunch between the magnetron anode and cathode.

The simulation results suggest that the output power, which is also correlated with the filament and frequency, increases with increasing anode current of the magnetron. Fig. 6 shows the anode-current dependence of the oscillating frequency and

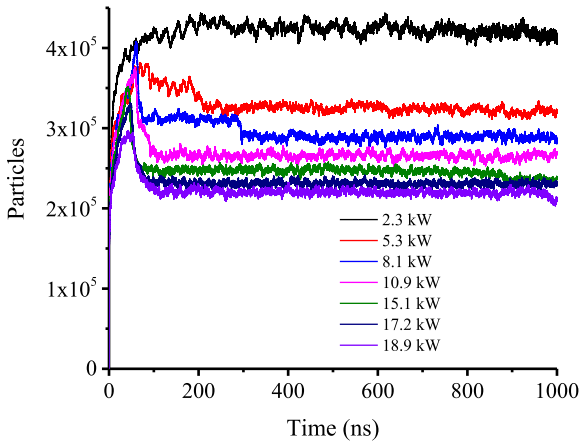

Fig. 7. Variation in the number of particles with output power.

the particle number in the free-running mode of the magnetron. With increasing output power, the frequency of the free-running magnetron shifts from 2.4387 to 2.4502 GHz.

Particle monitors are used to trace electron bunch formation and spokes formation during the simulations. The number of particles in the Anode-Cathode gap decreases with increasing output power (see Fig. 7), and at the same time, the output power increases when the anode current is adjusted. For a given π-mode stable oscillation, the spokes associated with electron bunch formation at 680 ns (Fig. 8) reveal that the number of particles in the resonator varies with the output power. Sharp spokes are obtained when the oscillation is set up, and the sharpness of these spokes increases with increasing output power.

The simulation results suggest that the operating current is correlated with the spoke position, when the magnetron is operated under constant electronic and magnetic fields. However, experimental verification of this correlation is difficult. The RF field in the interaction area intensifies and the radius of the Brillouin hub decreases with increasing output power and spoke height, respectively.

The Buneman-Hartree condition associated with the single-particle orbit model and Brillouin flow model of a conventional magnetron, describes the correlation among the operational voltage, magnetic field, electron velocity, and parameter of the magnetron structure [18], [19]; this parameter is unique. If the Hartree voltage (i.e., operational voltage) is kept constant, the frequency may be affected by the applied magnetic field. The Brillouin hub is rotated around the cathode, and may produce a ring current, which flows in the direction opposite to the rotation direction (see Fig. 9). Based on the magnetic fields generated by the electric current, the magnetic field stemming from the hub will vary slightly and the frequency varies with variations in the hub.

IV. Injection-Locking of Magnetron

If a magnetron is injection-locked by an external signal, the injection-locked bandwidth varies with varying output power, owing to magnetron-frequency pushing effects. We verified that this is the case by simulating a magnetron subjected to an injection signal. Once the magnetron is locked by this signal,

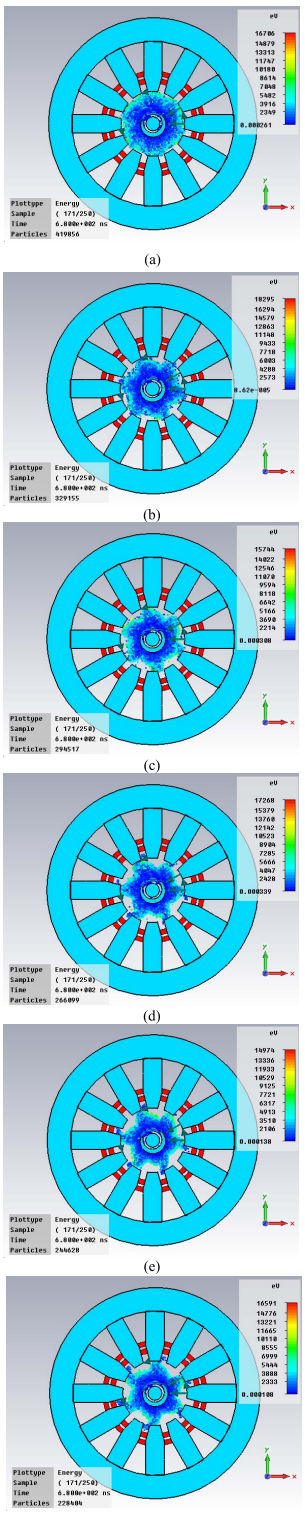

Fig. 8. Free-oscillation electron bunch formation at 680 ns and various values of the output power. (a) 2.3 kW. (b) 5.3 kW. (c) 8.1 kW. (d) 10.9 kW. (e) 15.1 kW. (f) 17.2 kW.

the injection-locked bandwidth varies with the magnetron output power.

When the magnetron is in free-running mode, the anode current and output power are 0.7 A and 5.3 kW, respectively. Figs. 10 and 11 show the spectrum and the corresponding number of particles obtained for free, unlocked, and locked statuses of the magnetron, respectively. When a 2.440-GHz

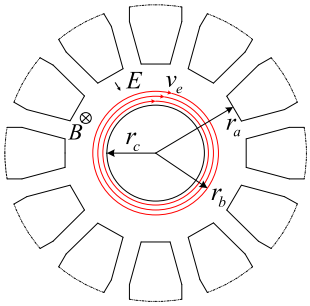

Fig. 9. Brillouin flow in the magnetron.

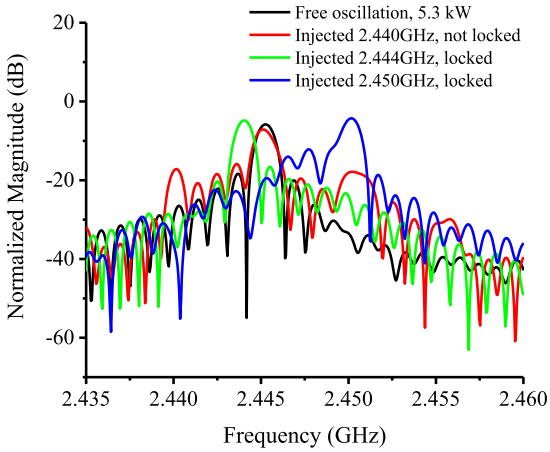

Fig. 10. Spectrum of the free, unlocked, and locked magnetrons, for a fixed output power of 5.3 kW.

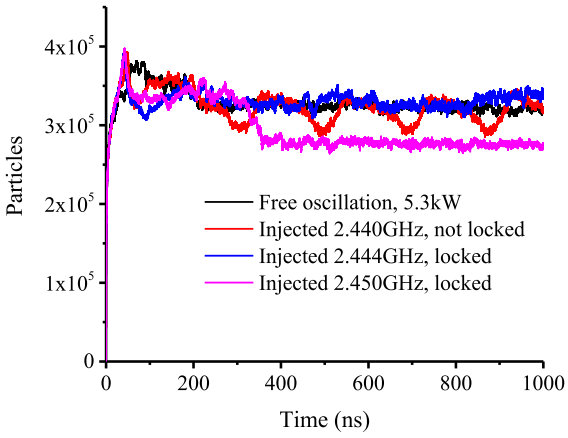

Fig. 11. Number of particles occurring under various conditions at a fixed power output of 5.3 kW.

signal is injected from the port at the end of the antenna, as shown in Fig. 1, the magnetron output frequency differs from 2.440 GHz, indicating that the magnetron is unlocked. An injected-signal frequency of 2.444 or 2.450 GHz yields a magnetron output frequency of 2.444 or 2.450 GHz, respectively. Moreover, as shown in Fig. 12, when the magnetron is locked at 2.450 GHz, the corresponding electron bunch formation is sharper than that occurring at 2.444 GHz.

At a magnetron anode current of ~1.8 A and an output power of 17.2 kW, the magnetron is strongly injection-locked between 2.450 and 2.451 GHz. Figs. 13 and 14 show the

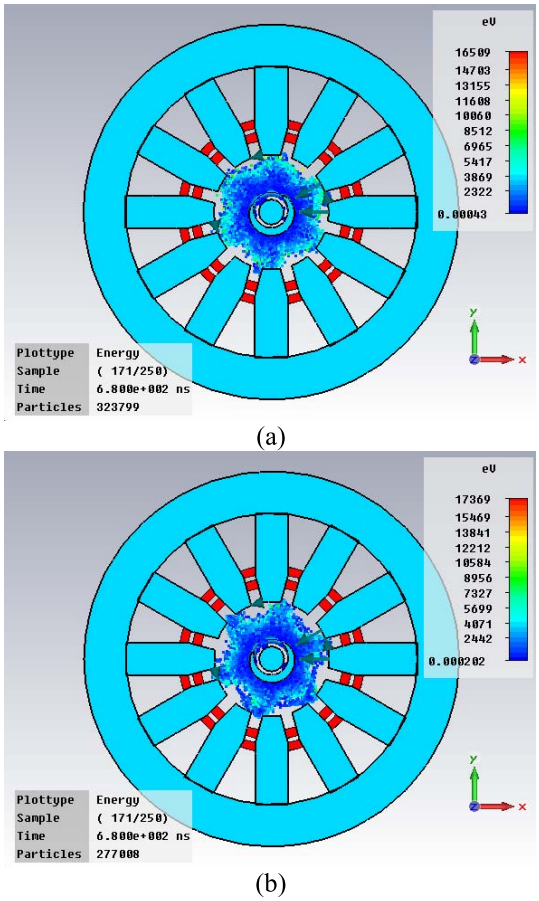

Fig. 12. Electron bunch formation of the injected signals (anode current: ~0.7 A). The upper and lower images correspond to the injection-locked magnetron at 2.444 and 2.450 GHz, respectively. The amplitude of the injected signals is constant.

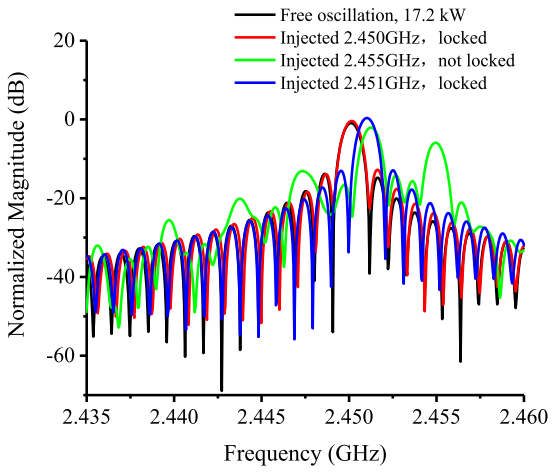

Fig. 13. Spectrum of the free, unlocked, and locked magnetrons for a given power output of 17.2 kW.

spectrum and number of particles in the electron bunch, respectively, associated with the free, unlocked, and locked configurations of the magnetron. The corresponding electronic bunch formation is shown in Fig. 15. The magnetron remains unlocked even after injection by a 2.455-GHz signal.

When the magnetron is injection-locked at 2.450 GHz, the Brillouin hub in the magnetron varies with the operating anode current. If the magnetron operating voltage, magnetic field,

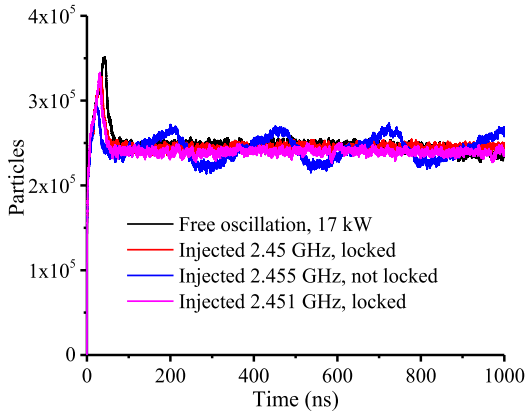

Fig. 14. Number of particles occurring under various conditions at a fixed output power of 17.2 kW.

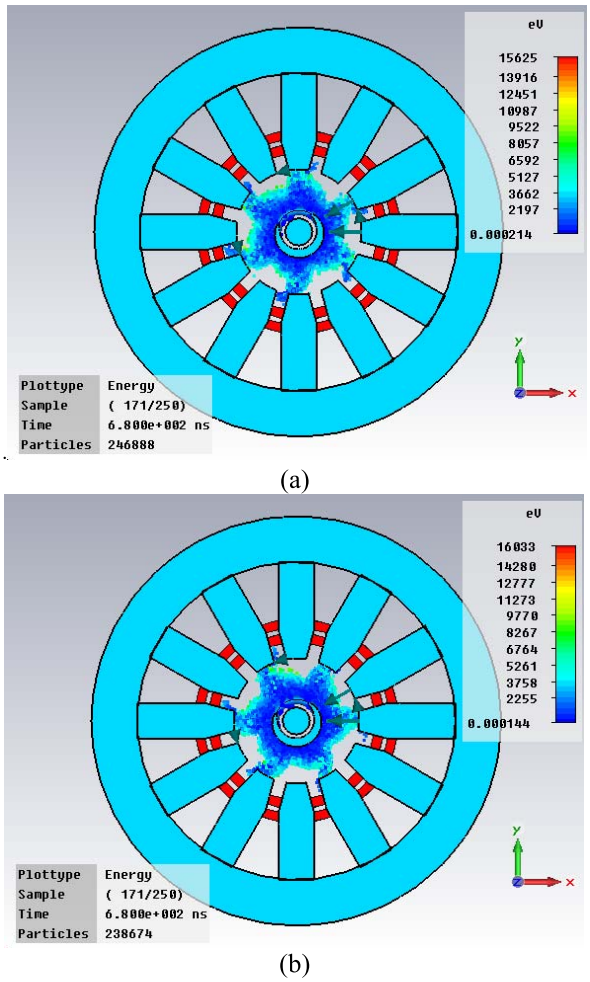

Fig. 15. Electron bunch formation of the injected signals (free-running output is 17.2 kW) for a magnetron injection-locked at (a) 2.450 GHz and (b) 2.451 GHz. The amplitude of the injected signals is constant.

and the operating current are known, then the height of the hub can be determined. The injected signal has more impact on the spokes than the hub. Additionally, the injection-locked bandwidth increases with decreasing output power.

When the magnetron output power is tuned, the injection-locked bandwidth scope varies. Table II shows the injection-locking experimental data, corresponding to magnetron output

TABLE II
INJECTION-LOCKED EXPERIMENT MEASUREMENTS RESULTS

Free-running Output Power (kW)	Injected Signal Power (W)	Output Power (kW)	Phase-locking Bandwidth Scope (GHz)	Injection-locked Bandwidth (MHz)
5.0	20	5.03	2.43917--2.44317	4.00
	60	5.20	2.43727--2.44491	7.64
	120	5.54	2.43488--2.44659	11.71
10.2	20	10.2	2.44794--2.44962	1.70
	60	10.3	2.44698--2.45044	3.46
	120	10.5	2.44619--2.45112	4.91
15.0	20	15.0	2.44967--2.4509	1.23
	60	15.1	2.4491--2.45132	2.22
	120	15.2	2.4485--2.45179	3.29
19.1	20	19.1	2.44987--2.4506	0.73
	60	19.1	2.4495--2.45105	1.55
	120	19.1	2.4491--2.4515	2.40

power values of 5, 10.2, 15, and 19.1 kW. In Table II, the output power is tuned from 5 to 19.1 kW, and the bandwidth decreases from 11.71 to 2.4 MHz, for a constant injection power of 120 W to the magnetron. Moreover, at high values of the output power, the center frequency of the phase-locked frequency scope shifts to a higher value, this is consistent with the occurrence of magnetron free-running frequency pushing effects.

V. CONCLUSION

A 3-D PIC model of a sector-and-slot side resonator magnetron is presented for investigating the behavior of the magnetron output and the particle variation in the magnetron cavity. The anode dc high voltage and the magnetic field are kept constant in the simulation and experiments, and we enhance the output power of the magnetron by increasing the anode current. With this improvement, a fixed-output-power industrial heating magnetron is transformed into a power-adjustable magnetron. For the first-time ever, the output microwave power of an injection-locked magnetron is continuously tuned from 2 to 19 kW in the free-running state. The frequency pushing phenomenon of a magnetron is observed in both the simulation and experiments. These effects increase the difficulty associated with injection-locking a magnetron, with widely varying output power, at a given frequency. In the simulation, the height of the electron spokes increases with increasing output power. Furthermore, preliminary studies of the phenomena associated with electron bunch formation were performed by adjusting the anode current of the magnetron. Injection-locking by an external signal is simulated with the 3-D model. This model will be helpful for theoretical investigations of an injection-locked magnetron. In the future work, we will consider the coherent power combining of the high power-adjustable phase-locked magnetrons.

REFERENCES

[1] A. S. Gilmour, *Klystrons, Traveling Wave Tubes, Magnetrons, Crossed-field Amplifiers, and Gyrotrons*. Norwood, MA, USA: Artech House, 2011.

[2] P. Pengvanich, *Theory of Injection Locking and Rapid Start-Up of Magnetrons, and Effects of Manufacturing Errors in Terahertz Traveling Wave Tubes*. Ann Arbor, MI, USA: Univ. Michigan, 2007.

[3] J. Achard *et al.*, "High quality MPACVD diamond single crystal growth: High microwave power density regime," *J. Phys. D, Appl. Phys.*, vol. 40, no. 20, p. 6175, 2007.

[4] H. Matsumoto, "Research on solar power satellites and microwave power transmission in Japan," *IEEE Microw. Mag.*, vol. 3, no. 4, pp. 36–45, Dec. 2002.

[5] N. Shinohara and H. Matsumoto, "Research on magnetron phased array with mutual injection locking for space solar power satellite/station," *Elect. Eng. Jpn.*, vol. 173, no. 2, pp. 21–32, 2010.

[6] G. Kazakevich *et al.*, "High-power magnetron transmitter as an RF source for superconducting linear accelerators," *Nucl. Instrum. Methods Phys. Res. A, Accel., Spectrom., Detect. Assoc. Equip.*, vol. 760, pp. 19–27, Oct. 2014.

[7] T. A. Treado, T. A. Hansen, and D. J. Jenkins, "Power-combining and injection-locking magnetrons for accelerator applications," presented at the IEEE Conf., Particle Accel., 1991.

[8] J. Benford, R. R. Smith, H. Sze, B. Harteneck, and W. Woo, "Phase-locking of relativistic magnetrons," *Proc. SPIE*, vol. 873, pp. 23–27, May 1988.

[9] S. C. Chen, G. Bekefi, and R. J. Temkin, "Operation of a long-pulse relativistic magnetron in a phase-locking system," in *Proc. Intense Microw. Particle Beams*, Los Angeles, CA, USA, 1990, pp. 36–43. [Online]. Available: http://proceedings.spiedigitallibrary.org/proceeding.aspx?articleid=937133

[10] T. A. Treado *et al.*, "Experimental results of power combining and phase-locking magnetrons for accelerator applications," in *Int. Tech. Dig. Electron Devices*, San Francisco, CA, USA, 1990, pp. 541–544.

[11] G. M. Kazakevich, V. M. Pavlov, Y. U. Jeong, and B. C. Lee, "Intrapulse frequency stability of a magnetron frequency-locked through a wave reflected from an accelerating cavity," *Nucl. Instrum. Methods Phys. Res. A, Accel. Spectrom. Detect. Assoc. Equip.*, vol. 647, pp. 10–16, Aug. 2011.

[12] G. Kazakevich *et al.*, "Magnetron RF source for the project X pulsed linac," Fermi Nat. Accel. Lab. (FNAL), Batavia, IL, USA, Tech. Rep., 2012.

[13] S. Sasaki, K. Tanaka, and K.-I. Maki, "Microwave power transmission technologies for solar power satellites," *Proc. IEEE*, vol. 101, no. 6, pp. 1438–1447, Jun. 2013.

[14] N. Shinohara and H. Matsumoto, "Phased array technology with phase and amplitude controlled magnetron for microwave power transmission," in *Proc. 4th Int. Conf. Solar Power Space (SPS)*, 2004, pp. 117–124.

[15] I. Tahir, A. Dexter, and R. Carter, "Noise performance of frequency- and phase-locked CW magnetrons operated as current-controlled oscillators," *IEEE Trans. Electron Devices*, vol. 52, no. 9, pp. 2096–2103, Sep. 2005.

[16] C. Liu, H. Huang, Z. Liu, F. Huo, and K. Huang, "Experimental study on microwave power combining based on injection-locked 15-kW *S*-band continuous-wave magnetrons," *IEEE Trans. Plasma Sci.*, vol. 44, no. 8, pp. 1291–1297, Aug. 2016.

[17] T. Isenlik and K. Yegin, "Tutorial on the design of hole-slot-type cavity magnetron using CST particle studio," *IEEE Trans. Plasma Sci.*, vol. 41, no. 2, pp. 296–304, Feb. 2013.

[18] D. H. Simon, Y. Y. Lau, J. W. Luginsland, and R. M. Gilgenbach, "An unnoticed property of the cylindrical relativistic Brillouin flow," *Phys. Plasmas*, vol. 19, no. 4, p. 043103, Apr. 2012.

[19] D. H. Simon, Y. Y. Lau, G. Greening, P. Wong, B. Hoff, and R. M. Gilgenbach, "Stability of Brillouin flow in the presence of slow-wave structure," *Phys. Plasmas*, vol. 23, no. 9, p. 092101, 2016.

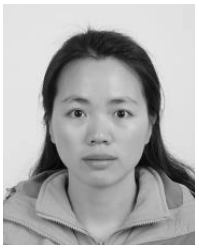

Heping Huang received the B.S. degree in communication engineering and the M.S. degree in circuit and system from the College of Physics and Information Science, Hunan Normal University, Changsha, China, in 2010 and 2013, respectively. She is currently pursuing the Ph.D. degree in radio physics with the School of Electronics and Information Engineering, Sichuan University, Chengdu, China.

Her current research interests include the practical simulation and experimental measurements of microwave magnetrons.

Yu Wei received the B.S. degree in physics from the College of Physics and Electronic Engineering, XinYang Normal University, Xinyang, China, in 2013. He is currently pursuing the master's degree in radio physics with the School of Electronics and Information Engineering, Sichuan University, Chengdu, China.

His current research interests include experimental control system of microwave magnetrons.

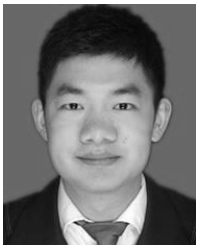

Xiaojie Chen received the B.S degree in information counter technology from the College of National Defense Science and Technology, Southwest University of Science and Technology, Mianyang, China, in 2014. He is currently pursuing the master's degree in radio physics with the School of Electronics and Information Engineering, Sichuan University, Chengdu, China.

His current research interests include the microwave engineering.

Kama Huang (M'01–SM'04) was born in Chongqing, China, in 1964. He received the M.S. and Ph.D. degrees in microwave theory and technology from the University of Electronic Science and Technology, Chengdu, China, in 1988 and 1991, respectively.

Since 1994, he has been a Professor with the School of Electronics and Information Engineering, Sichuan University, Chengdu, Sichuan, China. He has authored over 100 papers. His current research interests include microwave chemistry and electromagnetic theory.

Dr. Huang received several research awards from the Chinese government.

Changjun Liu (M'07–SM'09) received the B.S. degree in applied physics from Hebei University, Baoding, China, in 1994, the M.S. degree in radio physics and the Ph.D. degree in biomedical engineering from Sichuan University, Chengdu, China, in 1997 and 2000, respectively.

From 2000 to 2001, he was a Post-Doctoral Researcher at Seoul National University, Seoul, South Korea. From 2006 to 2007, he was a Visiting Scholar at Ulm University, Ulm, Germany. Since 1997, he has been with the Department of Radio-Electronics, Sichuan University, where he has been a Professor since 2004. He has authored one book, one chapter in a book, and more than 100 articles, and holds more than ten patents. His current research interests include microwave power combining of large-power vacuum components, microwave wireless power transmission, and microwave power industrial applications.

Prof. Liu received several honors such as the Outstanding Reviewer of the IEEE TRANSACTIONS ON MICROWAVE THEORY AND TECHNIQUES from 2006 to 2010, support from the MOE under the Program for New Century Excellent Talents in University, China from 2012 to 2014, a recipient of the Sichuan Province Outstanding Youth Fund from 2009 to 2012, and named by Sichuan Province as an Expert with Outstanding Contribution from 2008 to 2013. He serves on the Editorial Board of the Chinese journal Applied Science.